

# Resonant transmission in the base/collector junction of a bipolar quantum-well resonant-tunneling transistor

A. C. Seabaugh, Y.-C. Kao, W. R. Frensley, J. N. Randall, and M. A. Reed  
Central Research Laboratories, Texas Instruments Incorporated, Dallas, Texas 75265

(Received 10 June 1991; accepted for publication 16 October 1991)

A new transistor effect is demonstrated in a 120 nm base, bipolar quantum-well, resonant-tunneling transistor (BiQuaRTT). In this BiQuaRTT, a strong, multiple negative differential resistance (NDR) characteristic is obtained at room temperature with high-current gain ( $> 50$ ). The effect is shown to be the consequence of an asymmetric, quantum-well-base heterostructure whose shape is controlled by the base/collector bias. Changes in the quantum-well shape lead to large modulations of the transmission coefficient for quasi-thermalized minority electrons crossing the quantum-well base. In this letter, we describe the transport characteristics of these transistors, including also temperature and magnetic field dependence.

The bipolar quantum-well, resonant-tunneling transistor (BiQuaRTT) is a heterojunction, bipolar transistor with the quasi-neutral base region quantized by emitter/base and base/collector barriers.<sup>1,2</sup> In this paper, we show that strong room-temperature, size-quantization effects can be obtained in the BiQuaRTT with high-current gain at resonance and with wide quantum wells.<sup>3</sup>

The computed energy-band diagram<sup>4</sup> for the BiQuaRTT is shown in Fig. 1. This BiQuaRTT has a quantum-well width of 120 nm, with doping confined to the central 80 nm of the well. Note, that as a result of the undoped layer preceding the collector tunnel barrier, a triangular potential well forms at the base/collector junction [Fig. 1(a)], thereby making the quantum-well base asymmetric. The shape of the triangular well, particularly its depth, is controlled by the base/collector bias,  $V_{BC}$ , which in Fig. 1(a) is 0.5 V.

The basic heterostructure was grown on InP (Fe-doped) substrates in a Riber 2300 molecular beam epitaxy system. Starting from the substrate, the growth sequence was the following: 1  $\mu\text{m}$   $n^+$   $\text{In}_{0.53}\text{Ga}_{0.47}\text{As}$  collector contact layer ( $5 \times 10^{18} \text{ cm}^{-3}$ ), 150 nm  $\text{InGaAs}$  collector ( $2 \times 10^{16} \text{ cm}^{-3}$ ), 1.5 nm  $\text{AlAs}$  tunnel barrier, 20 nm undoped  $\text{InGaAs}$ , 80 nm  $p^+$  base (Be-doped  $5 \times 10^{18} \text{ cm}^{-3}$ ), 20 nm undoped  $\text{InGaAs}$ , 1.5 nm  $\text{AlAs}$  tunnel barrier, 50 nm quaternary  $\text{In}_{0.5}(\text{Ga}_{0.5}\text{Al}_{0.5})_{0.5}\text{As}$  emitter ( $2 \times 10^{18} \text{ cm}^{-3}$ ), 40 nm graded layer to  $\text{In}_{0.52}\text{Al}_{0.48}\text{As}$  ( $5 \times 10^{18} \text{ cm}^{-3}$ ), 40 nm graded layer from  $\text{InAlAs}$  to  $\text{InGaAs}$ , and finally, a 320 nm emitter contact layer ( $5 \times 10^{18} \text{ cm}^{-3}$ ). The  $\text{In}(\text{GaAl})\text{As}$  emitter injects electrons into the base at energies below the  $\Gamma$ -L intervalley transfer energy in  $\text{InGaAs}$ ; the  $\text{InAlAs}$  pre-emitter layer is included to increase the emitter injection efficiency.<sup>5</sup> The  $\text{InAlAs}$  emitter prelayer was removed in a second set of transistor growths without loss of the multiple negative differential resistance (NDR) characteristic.

The transmission coefficient, Fig. 1(b), is calculated from a solution of Schrödinger's equation in the envelope approximation, using the potential profile of Fig. 1(a). For energies below the allowed transmission energies, the structure resonances are determined from the derivative of

the wave-function phase with energy,  $d\theta/dE$ , shown on the lower axis of Fig. 1(b). Reflection resonances are the result of  $2\pi$  phase changes in the wave function with energy. Because of the 120-nm-wide quantum well, the lower transmission resonances in this structure are on the order of  $kT$  at room temperature.

A set of four transistors was fabricated based on the structure shown in Fig. 1, differing by the presence or absence of one or both of the  $\text{AlAs}$  tunnel barriers. Specifically, the first transistor utilized the BiQuaRTT structure of Fig. 1. A second transistor excluded both tunnel barriers, thereby forming a conventional  $\text{In}(\text{GaAl})\text{As}/\text{InGaAs}$  heterojunction bipolar transistor (HBT). A third transistor omitted the collector tunnel barrier, thus forming a tunnel barrier emitter HBT, and the final structure omitted the emitter tunnel barrier, thereby forming an HBT with a tunnel barrier at the base/collector junction. In this latter transistor, the base is quantized, so, it is also by our definition, a BiQuaRTT.

Strong multiple negative differential resistance (NDR)

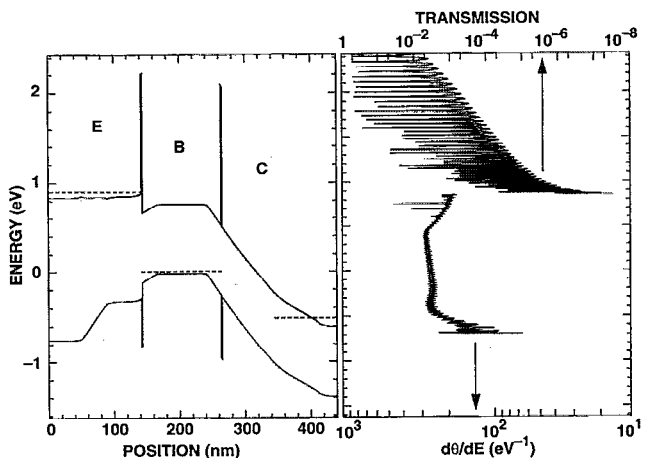


FIG. 1. (a) Computed potential profile for the BiQuaRTT at room temperature with  $V_{BE} = 0.95$  V, and  $V_{CB} = 0.5$  V. The dashed lines indicate the quasi-Fermi level energies which are set by the applied voltages. (b) The transmission and reflection resonances are computed from the potential profile of (a).

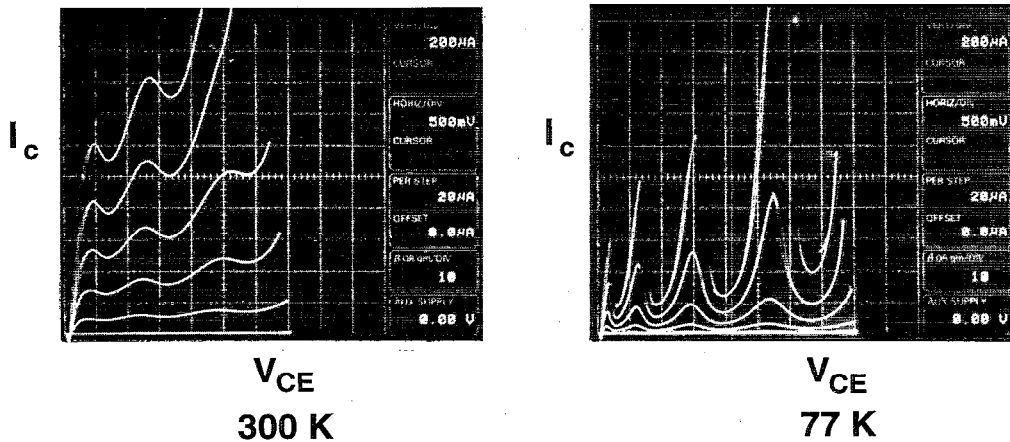


FIG. 2. Typical common-emitter transistor characteristics for the BiQuaRTT structure (cf. Fig. 1 excluding base/emitter tunnel barrier): (a) room temperature, and (b) 77 K. The emitter size of this device is  $2 \times 10 \mu\text{m}^2$ .

regions are observed in the two transistors which include the base/collector tunnel barrier, while in the conventional HBT and tunnel-emitter HBT structures, no NDR is observed. Typical room-temperature common-emitter transistor characteristics are shown in Fig. 2(a) for the BiQuaRTT which excludes the emitter/base tunnel barrier. Three NDR regions are clearly visible. The biases, current gain, and collector current magnitude are comparable for the entire set of transistors. From this set of four structures, it is apparent that the NDR is independent of the emitter tunnel barrier and requires the base/collector tunnel barrier.

When the device is immersed in liquid N [Fig. 2(b)], the resonances sharpen significantly, and the current gain is drastically reduced at the off-resonance biases. Note also that the first resonance at  $V_{CE} = 500 \text{ mV}$  in Fig. 2(a) is resolved into two resonances at 77 K [Fig. 2(b)].

These observations are explained as follows: minority electrons injected into the base have an energetic distribution exceeding the separation of quantized-base states. As the injected electrons diffuse across the base, they quasi-thermalize, and thereby assume a narrow distribution near the triangular potential well at the base/collector junction. As the base/collector bias increases, the lowest lying quantum-well base state with wave vector normal to the base/collector tunnel barrier is successively dropped into the triangular potential well, and is then below the energy of the narrow electron distribution at the emitter side of the triangular potential well. When this lowest lying state is dropped into the triangular well, the electrons are distributed amongst higher momentum states with lower transmission probability. The transmission probability is reduced because the tunnel barrier thickness is greater for the higher momentum states. This modulation of the transmission probability as states are dropped into the triangular potential well produces the NDR.

The common base characteristics are shown in Fig. 3, where it can be seen that the collector/base biases corresponding to the current peaks occur both for positive and negative bias polarities. For an emitter current here of  $200 \mu\text{A}$ , four resonances are apparent at low temperatures for  $V_{CB} = -0.70, -0.28, 0.51,$  and  $1.72$ . Note that the first resonance occurs for a collector/base voltage correspond-

ing to a nearly flatband base/collector condition. We also note from Fig. 3 that the current transfer ratio,  $\alpha$ , increases at the resonant peaks, resulting in an increase in the current gain. The arrows denote the computed resonance conditions, as described next.

A calculation of the quasi-bound states in the triangular potential well as a function of the base/collector bias is shown in Fig. 4. The horizontal dashed line represents the conduction-band energy in the neutral  $p$ -type base, and corresponds to the lowest injection energy for minority electrons into the triangular potential well. The quasi-bound states of the triangular well are estimated from the eigenfunction for the infinite barrier triangular well,<sup>6</sup>

$$E_n = \left( \frac{\hbar^2}{2m} \right)^{1/3} \left( \frac{3\pi a}{2} \right)^{2/3} \left( n + \frac{3}{4} \right)^{2/3} \quad n=0,1,2,\dots, \quad (1)$$

where  $\hbar$  is Planck's constant,  $m$  is the effective mass,  $a$  is the slope of the triangular well in eV per unit length, and  $n$  is the quantum number. In the BiQuaRTT, the parameter  $a$  is a function of the base/collector bias  $V_{BC}$ , and has been determined from self-consistent calculations of the band profile for this BiQuaRTT heterostructure, and is fit by the relation  $a = 7.91 V_{CB} + 6.3 \text{ eV}/\mu\text{m}$ . Using this relation and Eq. (1), the eigenvalue positions can be estimated. The resonance conditions occur when the triangular well depth

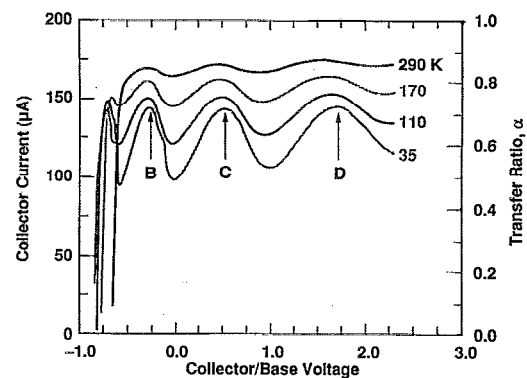


FIG. 3. Temperature-dependence of the common-base transistor characteristics for the BiQuaRTT structure (cf. Fig. 1 excluding base/emitter tunnel barrier) with  $I_E = 200 \mu\text{A}$  and emitter size of  $12 \mu\text{m}^2$ . The arrows denote the computed resonance biases.

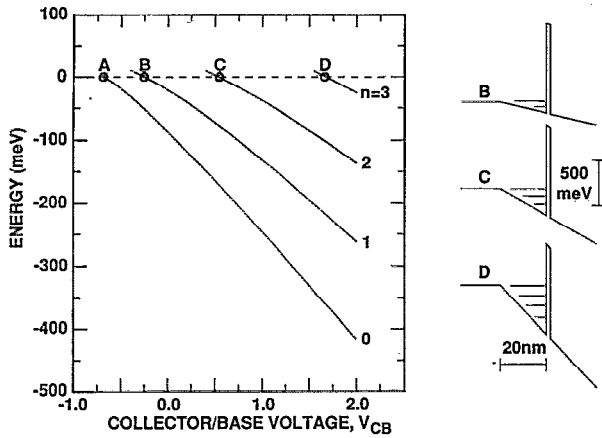


FIG. 4. Calculated dependence of the triangular potential-well subband energies as a function of the base/collector voltage. The subband energies are defined with respect to the conduction-band minimum in the  $p$ -type base.

is just such that a state is present at the top of the well, i.e., at the energy  $ad$ , where  $d$  is the well thickness of 20 nm. We find that, with only minor adjustment of the  $a$  ( $V_{CB}$ ) relation, i.e.,  $a = 10 V_{CB} + 8 \text{ eV}/\mu\text{m}$ , that remarkable agreement is found between theory and experiment, as shown by the arrows in Fig. 4.

For the biases shown in Figs. 3 and 4, it can be seen that the effect of the base/collector bias is to successively lower the quasi-bound states through the minority electron distribution in the base. The density of states for electrons with wave vector normal to the base/collector tunnel barrier alternately increases and decreases with this monotonically increasing base/collector bias. From this calculation, we observe four states passing below the electron quasi-Fermi energy, in close agreement with the four resonances we observe in Fig. 3. The first resonance position, not labeled, is predicted to occur for biases slightly less than the base/collector flatband bias, i.e.,  $E_g/q = 0.78 \text{ V}$ , where  $E_g$  is the bandgap energy of InGaAs, and  $q$  is the fundamental charge.

Also consistent with this model, when a magnetic field is applied parallel to the current transport direction, an increase in the current at resonance is observed. Shown in Fig. 5, the collector current in the transistor under constant base bias current increases by as much as a factor of 660 with increasing magnetic field. This is qualitatively consistent with an increase in the density-of-states associated with the formation of Landau levels in the base, but its magnitude is surprising. The apparent splitting of the second peak is due to circuit oscillation in the NDR region. The magnetic field dependence was also examined for  $B$  perpendicular to  $J$ . As expected, this field orientation results in an increase in base scattering and a monotonic decrease in the magnitude of the collector current peaks.

A second set of three transistors was grown to further test the transport model. The first control transistor structure reproduced the multiple NDR effect, while differing from the device of Fig. 1 in that it had no InAlAs emitter layer or emitter/base tunnel barrier, and the 20 nm un-

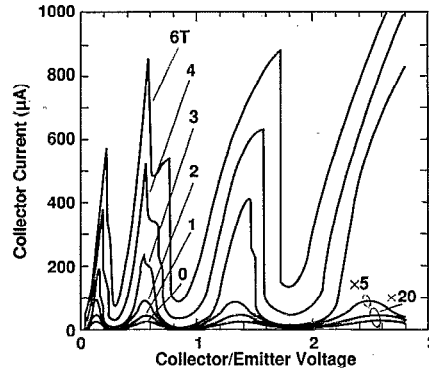


FIG. 5. Magnetic-field dependence of the collector current for  $I_B = 25 \mu\text{A}$  for  $J$  parallel to  $B$ : same device as in Fig. 3, temperature 4.2 K.

doped spacer layer on the emitter side of the Be-dopants was eliminated, thereby reducing the quantum-well base to 100 nm. A second transistor was designed to eliminate the multiple NDR effect by removing the emitter/base heterostructure. Without the emitter/base heterojunction, the base has no size quantization above the triangular potential well energy, and there is, then, no wave vector selection with base/collector bias. As expected, no NDR is observed in this second transistor. A third transistor was grown in which the formerly undoped spacer at the base/collector junction is doped with Be. The multiple NDR effect is then eliminated without the presence of the triangular potential well. In addition, we note that the gain in this latter transistor is reduced (to near unity) due to the increased AIAs barrier height with respect to the minority electrons, causing increased reflection and a greatly reduced base transport factor.

In conclusion, we have realized strong room-temperature current modulation with high current gain ( $> 50$ ) in a 120 nm base BiQuaRTT. This new effect is shown to be the consequence of an asymmetric quantum-well-base heterostructure, whose shape is controlled by the base/collector bias. Changes in the quantum-well shape lead to large modulation of the transmission coefficient for quasi-thermalized minority electrons. The transmission resonances are in remarkable agreement with calculation.

The authors gratefully acknowledge support by the Air Force Wright Laboratories, Contract No. F33615-89-C-1074. We also acknowledge useful discussions with R. T. Bate, J. H. Luscombe, and H.-T. Yuan, and the excellent technical support of P. Stickney, R. Aldert, R. Thomason, B. Garmon, F. Goodman, and P. Williams.

<sup>1</sup> M. A. Reed, W. R. Frensley, R. J. Matyi, J. N. Randall, and A. C. Seabaugh, *Appl. Phys. Lett.* **54**, 1034 (1989).

<sup>2</sup> A. C. Seabaugh, W. R. Frensley, J. N. Randall, M. A. Reed, D. L. Farrington, and R. J. Matyi, *IEEE Trans. Electron Devices* **36**, 2328 (1989).

<sup>3</sup> A. C. Seabaugh, Y.-C. Kao, W. R. Frensley, J. N. Randall, and M. A. Reed, 1990 Device Research Conference Abstracts, Santa Barbara, CA.

<sup>4</sup> J. H. Luscombe and W. R. Frensley, *Nanotechnology* **1**, 131 (1990).

<sup>5</sup> L. F. Luo, H. L. Evans, and E. S. Yang, *IEEE Trans. Electron Devices* **36**, 1844 (1989).

<sup>6</sup> S. Flügge, *Practical Quantum Mechanics I* (Springer-Verlag, Berlin, 1971), p. 101.